Iranian Biomedical Journal 10 (4): 215-223 (October 2006)

Fabrication of Porous Hydroxyapatite-Gelatin Composite Scaffolds for Bone Tissue Engineering

Mehdi Kazemzadeh Narbat*[1], Fariba Orang[2], Mehran Solati Hashtjin[2] and Azadeh Goudarzi[2]

[1]*Science and Research University, P.O. Box 147676698;* [2]*AmirkabirUuniversity of Technology, P.O. Box 15875-4413, Tehran, Iran*

Received 25 December 2005; revised 17 July 2006; accepted 17 July 2006

ABSTRACT

Background: engineering new bone tissue with cells and a synthetic extracellular matrix represents a new approach for the regeneration of mineralized tissues compared with the transplantation of bone (autografts or allografts). **Methods:** in this study, to mimic the mineral and organic component of natural bone, hydroxapatite (HA) and gelatin (GEL) composite scaffolds were prepared. The raw materials were first compounded and the resulting composite were molded into cylindrical shape. Using solvent-casting method combined with freeze drying process, it is possible to produce scaffolds with mechanical and structural properties close to natural trabecular bone. Glutaraldehyde (GA) was used as cross linking agent. The chemical bonding and the microstructure were investigated by Fourier Transform Infra Red (FT-IR), Scanning Electron Microscopy (SEM) and Light microscopy. **Results:** it was observed that the prepared scaffold has an open, interconnected porous structure with a pore size of 80-400 μm, which is suitable for osteoblast cell proliferation. The mechanical properties of different weight fraction of HA (30, 40, and 50 wt%) was assessed and it was found that the GEL/HA with ratio of 50wt% HA has the compressive modulus of ~10 Giga Pascal (GPa), the ultimate compressive stress of ~32 Mega Pascal (MPa) and the elongation of ~3MPa similar to that of trabecular bone. The porosity and the apparent density of 50wt% HA scaffold were calculated and it was found that the addition of HA content can reduce the water absorption and the porosity. Since GA is cytotoxin, sodium bisulfite was used as GA discharger. The biological responses of scaffolds carried out by L929 fibroblast cell culture and it was observed that fibroblast cells partially proliferated and covered scaffold surface, 48h after seeding. **Conclusion:** these results demonstrate that the manufactured scaffolds are suitable candidate for trabecular bone tissue engineering. *Iran. Biomed. J. 10 (4): 215-223, 2006*

Keywords: Scaffolds, Hydroxyapatite (HA), Bone tissue engineering

INTRODUCTION

Tissue engineering offers a new promising approach to the creation of biological alternatives for implants and prostheses [1]. Bone tissue is considered as minerals and proteins. The minerals are mostly apatites such as hydroxyapatite (HA, Ca_{10} $(PO_4)_6(OH)_2$), fluorapatite and carbonate-apatite [2]. In general, HA is a main component of bone mineral and in some cases carbonate-apatite is a main hard tissue component, as in dental enamel [3]. HA is widely accepted as a bioactive material for guided regeneration [4].

HA has excellent biocompatibility with hard tissues [5, 6], and high osteoconductivity and bioactivity despite its low degradation rate, mechanical strength and osteoinductive potential [7, 8]. Calcified tissue such as long bone and jaw bone is considered a biologically and chemically bonded composite between HA and type-I collagen [9]. Collagen is biocompatible, biodegradable and osteoinductive, acting as an excellent delivery system for bone morphogenetic proteins [10, 11]. Gelatins (GEL) are compositionally virtually identical to the collagen from which they are derived. They have been shown to be biocompatible and resorbable.

GEL is readily assimilated by the body [12]. A composite scaffold of HA and GEL is therefore expected to show increased osteoconductivity and biodegradation together with sufficient mechanical

*Corresponding author; Tel. (+98 912) 1273667; Fax: (+98-262) 622 1888; E-mail: mehdikazemzadeh@yahoo.com

[Downloaded from ibj1.pasteur.ac.ir on 2026-10-20]

[DOR: 20.1001.1.1028852.2006.10.4.8.3]

strength [13]. One of the major problems in practice with type-I collagen is its cost and the poor definition of commercial sources of this material. Therefore in the present study, collagen type-I was replaced by GEL. To mimic the mineral and organic component of natural bone, a bone like scaffold composite can be produced by dispersing particulate HA throughout a GEL matrix. Most tissue engineering approaches to the restoration and repair of damaged tissues require a scaffold material upon which cells can attach, proliferate, and differentiate, into a functionally and structurally appropriate tissue for the body location into which it is placed [14].

Solvent casting is a simple method for fabricating constructs for tissue engineering. In this method, the polymer is dissolved in a suitable solvent and poured into a mold. The solvent is then removed, leaving the polymer set in the desired shape. The major goal in fabricating scaffolds for tissue regeneration is to accurately control pore size and porosity. By using Freeze-Drying method, the liquid state structure of composite is locked and the solvent is removed by rapidly cooling under vacuum [15, 16]. Glutaraldehyde (GA) can be used as cross-linking agent in the making of GEL-tricalcium phosphate composites rendering them no longer water soluble.

Although GA is known as a cytotoxin, its use as a cross-linking agent in the preparation of possible large bone substitutes was supposed [17] to be acceptable upon implantation evaluations. In any case residues of this agent can be removed by drying the treated material to 100°C, as well as by treatment with sodium bisulfite [18]. Our objective in this study is to characterize the prepared HA-GEL composites.

MATERIALS AND METHODS

Materials. The major materials were microbiological GEL (Merck Inc. 4070, Germany), bioceramic grade HA (Merck Inc. 2196, Germany) and deionized water (DI) as GEL solvent. A 25% solution of GA (Merck Inc. 2927, Germany) was used as crosslinking agent The KH_2PO_4 (BDH Chemicals Inc. 10203, Canada), $Na_2HPO_4.12H_2O$ (Merck Inc. 106573, Germany), KCl (Merck Inc. 4936, Germany) and NaCl (Merck Inc. 106400, Germany) were used for PBS (phosphate buffer saline) preparation.

Preparation of HA-GEL scaffolds. The slurry composite was prepared using solvent casting method [18]. As dry GEL is essentially intractable material, it can readily become castable or shapeable when transformed into a sol-GEL state by dissolution in water up to about 5-30 wt% [18]. In order to have a homogenous and strong composite, the HA particles finer than 75 μm were obtained using sieve with mesh no. 200. Definite GEL content 12.33 wt% was dissolved in DI at temperature of 45°C [18]. Then the 30 wt%, 40 wt% and 50 wt% HA contents were added to prepare three different composites. The progen can be added at this stage if needed. The reinforced slurry composite was then heat treated on magnet stirrer under constant mixing at 45°C for 1 h. The slurry was deagglomerated by magnet stirring. The temperature was monitored continuously. It should be noted that to make a well distributed homogenous composite, the heat must not be applied directly to the composite.

By using an interface water bath beaker, the heat treatment process can be homogenously applied to the reaction vessel. The slurry immediately was injected into cylindrical Teflon molds (12 mm in height and 6 mm in diameter) by using a syringe to avoid the air bubbles. The molds were frozen at -70°C and then dried in a commercial freeze-dryer for 6 h for solvent (DI) removal. After that, the white composites were removed and placed in room temperature for 24 h, and then they were immersed in an 8% solution of GA for 3 h. The cross linked composites have bright brown color. To remove the residues of GA agent, the cylinders were washed with DI for 24 h, during that time, the water was changed every 6 h. Besides, the sodium bisulfite was used to discharge the excessive GA. Since in freeze-drying technique a surface skin appears, to achieve the porous structure the surface of scaffolds were sand blasted. For statistical analysis in all assays, four samples of each type were investigated and the average was reported.

Characterization:

Fourier Transform Infra Red (FT-IR). In the present study, FT-IR spectroscopy (Thermo nicolet NEXUF870, USA) was used to estimate the conformational change of the structure in HA-GEL composites cross-linked by GA [3, 19, 20].

Compressive testing. One of the major problems for mechanical characterization of porous ceramic scaffolds is the difficulty in machining and gripping specimen; hence the conventional methods of mechanical characterization such as tensile, biaxial and impact testing are usually inapplicable to porous

[Downloaded from ibj1.pasteur.ac.ir on 2026-10-20]

[DOR: 20.1001.1.1028852.2006.10.4.8.3]

materials [21]. Instead, the compression test has been widely accepted and used successfully for characterization of cancellous bone and porous HA [22, 23].

The compressive strength, Young's modulus and elongation of composites were measured at 25°C. Scaffolds were tested with an Instron materials testing machine (model 1195, Instron Corp., UK) using a cross-head speed of 1 mm/min with a 1000N load cell. As mentioned before, the samples were cylinders of approximately 6 mm in diameter and 12 mm in height in accordance with the compression mechanical test guidelines set in American Standard Test and Measurement (ASTM F 451-95).

Water absorption. Water absorption of HA-GEL composites with different HA content were studied to evaluate the effect of HA content on the size and stability of material. The ratio of water absorption (W_a) at time *t* was calculated using the following equation:

$$W_a\% = \frac{W_t - W_0}{W_0} \times 100\% \qquad (1)$$

Where W_t and W_0 are the weights of sample at time *t* and the dry state at room temperature, respectively.

Measurement of porosity and density. A liquid displacement method was used to measure the porosity and density of 50wt% HA scaffold [24]. The density measurements provided information about pore size and distribution, permeability, and presence of structural faults in sintered ceramic structures [24]. A scaffold of weight W was immersed in a graded cylinder containing a known volume (V_1) of ethanol. The cylinder was placed in a vacuum to force the ethanol into the pores of the scaffold until no air bubble emerged from the scaffold. The total volume of the ethanol and scaffold was then recorded as V_2. The volume difference ($V_2 - V_1$) was the volume of the skeleton of the scaffold. The scaffold was removed from the ethanol and the residual ethanol volume was measured as V_3. The total volume of the scaffold, V, was then

$$V = V_2 - V_3 \qquad (2)$$

The apparent density of the scaffold, ρ was evaluated using,

$$\rho = \frac{W}{(V_2 - V_3)} \qquad (3)$$

The porosity of the open pores in the scaffold, ε was evaluated using [22],

$$\varepsilon = \frac{(V_1 - V_3)}{(V_2 - V_3)} \qquad (4)$$

Scanning electron microscopy (SEM). The morphology and microstructure of the scaffolds were examined using SEM LEO 440 i at 10 or 15 kV. The scaffolds were cut by a razor and polished and then were gold-sputtered (POLARION SC7610, USA).

Cell culture. The mouse L929 fibroblast cells were used as a test mode in this study. The cells were maintained in growth medium RPMI-1640 supplemented with 100 IU/ml penicillin, 100 μg/ml, streptomycin (Gibco BRL Laboratories, USA) and 10% FCS (Gibco BRL, USA). A routine subculture was used to maintain the cell line. The cells were incubated in a humidified atmosphere of 5% CO2 at 37°. The cell suspension of 4×10^5 cells/ml was prepared before seeding. The samples were sterilized in 70% alcohol and washed in culture medium before the cell seeding procedure. They were placed in a multi well tissue culture polystyrene 24 wells plate (Nunc, Denmark) with 1 ml cell suspension, with 4 wells kept as a negative control and then maintained in the incubator for 48 h. After incubation, the samples were removed from the incubator and washed immediately in PBS. The attached cells were determined using the image processing system (×100 magnification, Nikon ECLIPSE TE2000-U, Japon).

RESULTS AND DISCUSSION

Infrared analysis. The FT-IR spectrum of the GEL and 30 wt%, 40 wt% and 50 wt% HA-GEL composites are shown in Figure 1. The composite spectrums are similar to the spectra of real bone [3, 25, 26]. The band at 1337 cm^{-1} in GEL is attributed predominantly to the so-called wagging vibration of proline side chains. The 1337 cm^{-1} band in GEL does not simply represent the carboxyl group, but it is one of a number of bands in the range of 1400-1260 cm^{-1} which are attributed to the presence of type-I GEL [26, 27]. The amide A band arising from N-H stretching was distributed at 3270-3370 cm^{-1} relative to the degree of cross-linking, C-H

[Downloaded from ibj1.pasteur.ac.ir on 2026-10-20]

[DOR: 20.1001.1.1028852.2006.10.4.8.3]

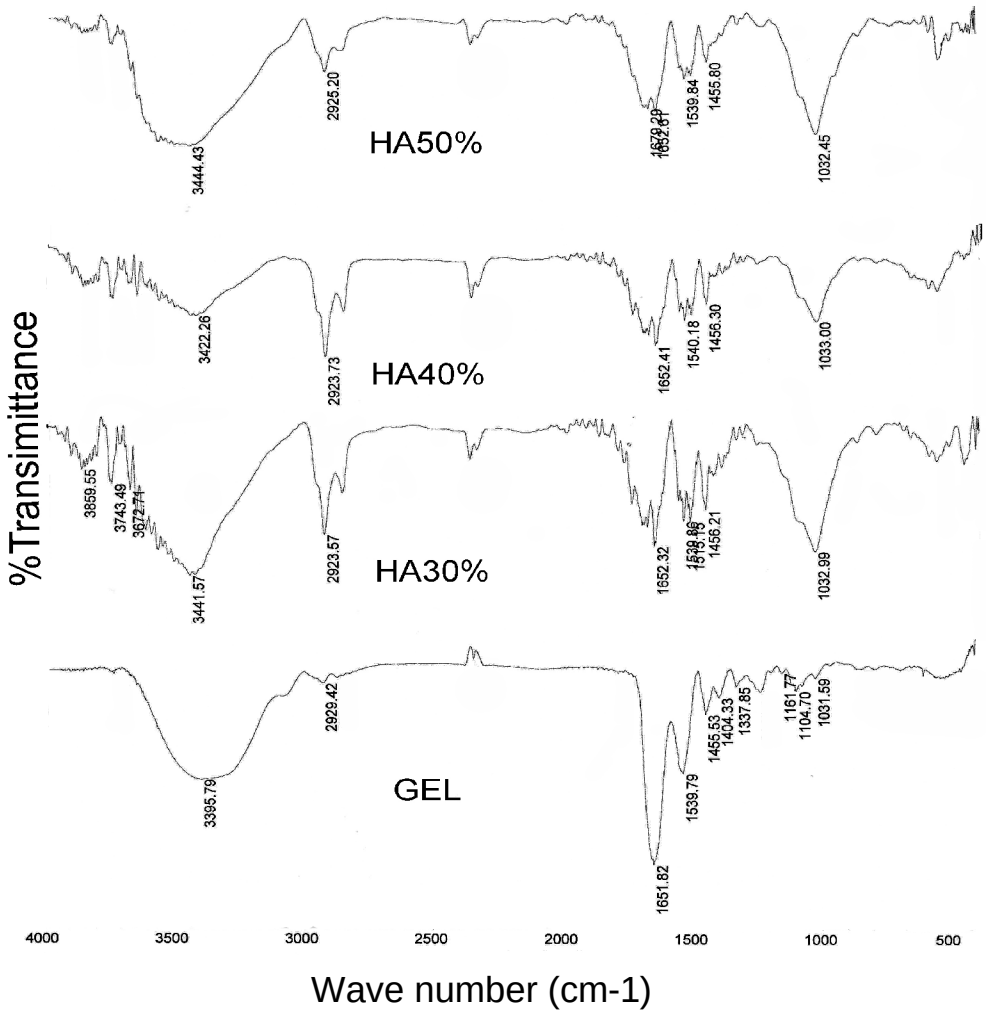

Fig. 1. FT-IR spectra for GEL and 30 wt%, 40 wt%, 50 wt% cross-linked HA-GEL composites.

stretching at ~2920 cm^{-1} for the amide B, C = O stretching at 1670-1650 cm^{-1} for the amide I, N-H deformation at 1500-1550 cm^{-1} for the amide II [26, 27]. The appearance of an amide I mode indicated that HA-GEL composites adopt a predominantly α-helical configuration and this is confirmed by the appearance of amide II at ~1540 cm^{-1} [28, 29]. As HA related bands, there are hydroxyl group (-OH) stretching (4000-3200 cm^{-1}) and liberational (~600 cm^{-1}) bands, and phosphate contours. There are CO_3 V_3 bands at 1580-1400 cm^{-1} and 1530-1320 cm^{-1}, and the carbonate V_2 band is located at 890-800 cm^{-1}. The phosphate band is between 900 and 1200 cm^{-1}. The shift of the 1337 cm^{-1} band in GEL has been effectively used to confirm the chemical bond formation between carboxyl ions in GEL and HA phases [25, 26, 28]. During the process of HA-GEL composite, the Ca^{2+} ions will make a covalent bond with R-COO^- ions of GEL molecules. Moreover the cross-linking induces the shortening of the distance between HA-GEL fibrils within the critical length and more amount of Ca^{2+} ions on HA will have a chance to bind with R-COO^- ions of GEL molecules [27-29].

Mechanical properties. The Young's module was defined by the slope of the initial linear portion of the stress-strain curve. The ultimate compressive strength was determined from stress-strain curve by applying the load until the scaffold was cracked. The compressive modulus of HA-GEL scaffolds increased with HA content (Fig. 2). The 30 wt%, 40 wt% and 50 wt% composites had compressive modulus of 2.3, 7.3 and 10.2 Giga Pascal (GPa),

[Downloaded from ibj1.pasteur.ac.ir on 2026-10-20]

[DOR: 20.1001.1.1028852.2006.10.4.8.3]

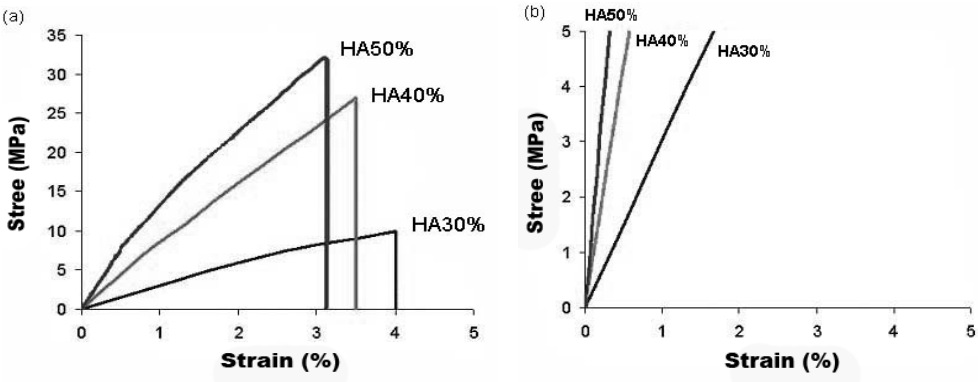

Fig. 2. (a), Typical stress-strain curves recorded for HA30%, HA40% and HA50% composites; **(b),** initial regions of the stress-strain curves.

respectively and the ultimate compressive strengths were 9.7, 25.6 and 32.1 Mega Pascal (MPa), respectively. For human trabecular bone, the maximum Young's modulus (E) belongs to the femoral head which is 900 ± 710 MPa with 9.3 ± 4.5 MPa compressive strength [30].

For the cortical bone, the maximum compressive E belongs to Tibia ranging 24.5-34.3 GPa with 166 MPa compressive strength [30]. The obtained ultimate elongation also varies from 3.1-4% which decreases with HA content. For human bone, compressive strain rates rang from -7000 to -34000 με/s which are normally about 2.9% [30].

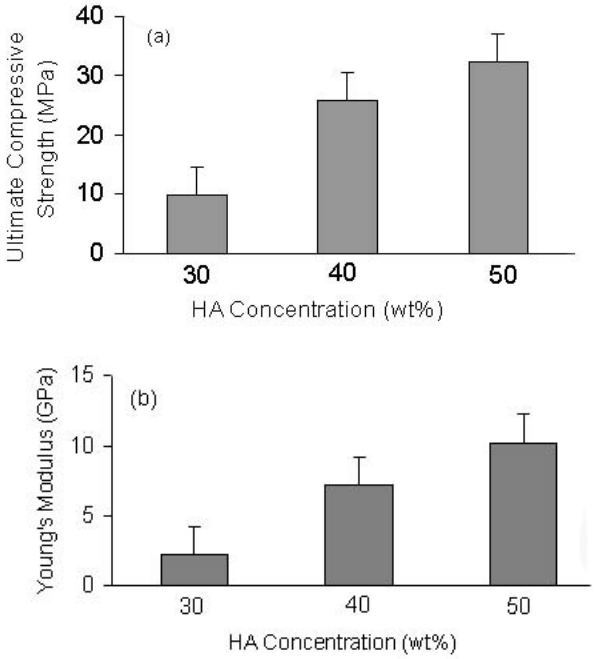

Fig. 3. Comparison of **(a)** ultimate compressive strength and **(b)** Young's modulus of different HA contents composites.

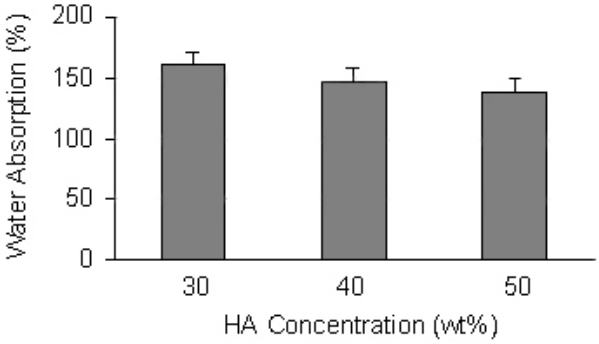

Fig. 4. Water absorption for different HA-GEL ratio.

Water absorption. The behavior of water absorption of HA-GEL composite was investigated, and results are shown in Figure 4. The water absorption reaches a highest point of about 150% after a week. The water absorption of HA-GEL composite reduces with HA content due to formation of a temporary HA barrier preventing water permeating into the scaffold.

Morphology. The morphology and microstructure of the scaffolds were examined using SEM and light microscopy (Figs. 6 and 7). It can be seen from Figures 6 and 7 that the pores in the scaffolds are interconnected and their sizes range from 80 to 400 μm. Since one osteoblast occupies an area of approximately 700 μm^2 [31], hence the pore size of 500 μm (diameter of a spherical pore) is compatible with osteoconduction [32], however the optimum pore size for osteoconduction is 150 μm [33]. This shows that the scaffolds' pores are sufficiently large to accommodate cells.

[Downloaded from ibj1.pasteur.ac.ir on 2026-10-20]

[DOR: 20.1001.1.1028852.2006.10.4.8.3]

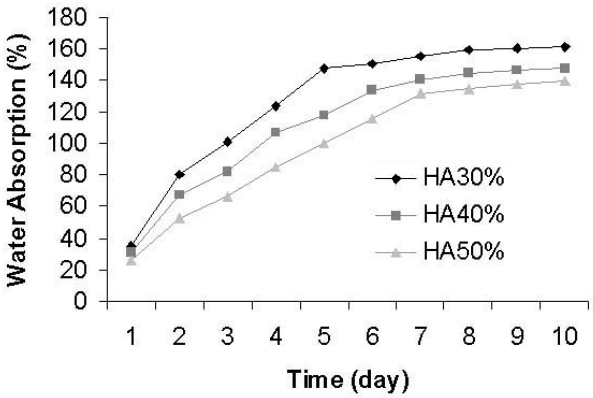

Fig. 5. Dependence of water absorption on time for different HA-GEL sample.

Porosity and density. The apparent density of a porous scaffold can influence its mechanical strength, permeability, and presence of structural defects [34]. The measured density and porosity of HA-GEL composite scaffolds prepared with slurries of different HA concentrations using the method shown before were 1.17 g/cm^3 and about 70%, respectively. The apparent density of trabecular bone ranges from 0.14 to 1.10 g/cm^3 (average: 0.62 ± 0.11 g/cm^3) [34].

Porosity characterization is based on the presence of open pores which are related to properties such as permeability and surface area of the porous structure. It was found from SEM image analysis that the addition of HA results in more dense and thicker pore walls with lower porosity, therefore the addition of HA content improves the mechanical properties [35, 36]. Since a higher density of a scaffold usually leads to higher mechanical strength while a high porosity provides a favorable biological environment, a balance between the porosity and density for a scaffold must be established for the specific application.

Cell attachment evaluation. Experiments of cell culture were carried out to test the biocompatibility of scaffolds. By using bisulfite sodium which is safe for biomedical use, the problem of residual cross-linking agent (GA) can be resolved. Rarely cellular degeneration or death was observed in the standard cytotoxicity assays of the biomaterial samples studied [37]. Cells exhibited rather good proliferation and partially covered the composite surface (Fig. 8).

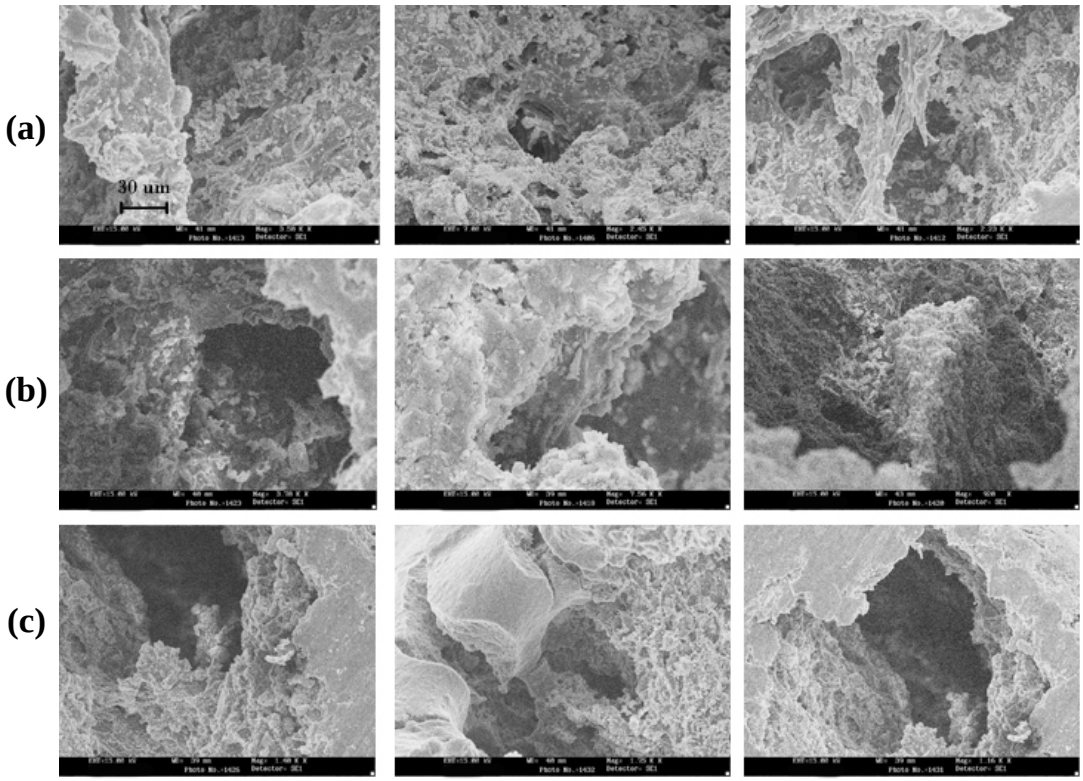

Fig. 6. SEM micrographs of pores in the cross-section of different HA-GEL scaffolds, raw **(a)** HA30%, raw **(b)** HA40%, raw **(c)** HA50%.

[Downloaded from ibj1.pasteur.ac.ir on 2026-10-20]

[DOR: 20.1001.1.1028852.2006.10.4.8.3]

In this work, a method of producing three dimensional, open-cells, composite scaffold of HA-GEL has been developed. The technique involves solvent-casting method combined with freeze drying process which has the advantages of both methods. The prepared scaffolds are porous, with porosity higher than 70% and have pores ranging from 80 to 400 µm. A compressive Young's modulus of 10.2 GPa, ultimate compressive strength of 32.1 MPa and the apparent density of 1.17 g/cm^3 for the scaffold with HA concentration of 50 wt% were achieved which are comparable to that of trabecular bone. FT-IR spectrum for the cross-linked HA-GEL composite indicates chemical bond formation between carboxyl ions in GEL and HA phases. The addition of HA can reduce the water absorption. The scaffolds exhibited good tissue compatibility to L929 fibroblast cell culture. It was observed that cells cultured in scaffolds could attach, spread, and proliferate well.

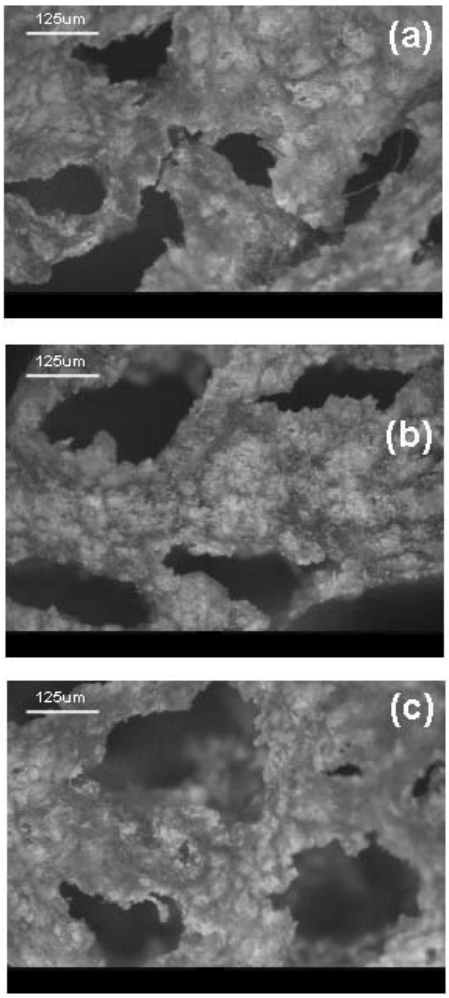

Fig. 7. Morphology of the composite scaffolds under light microscopy **(a)** HA30% **(b)** HA40% **(c)** HA50%.

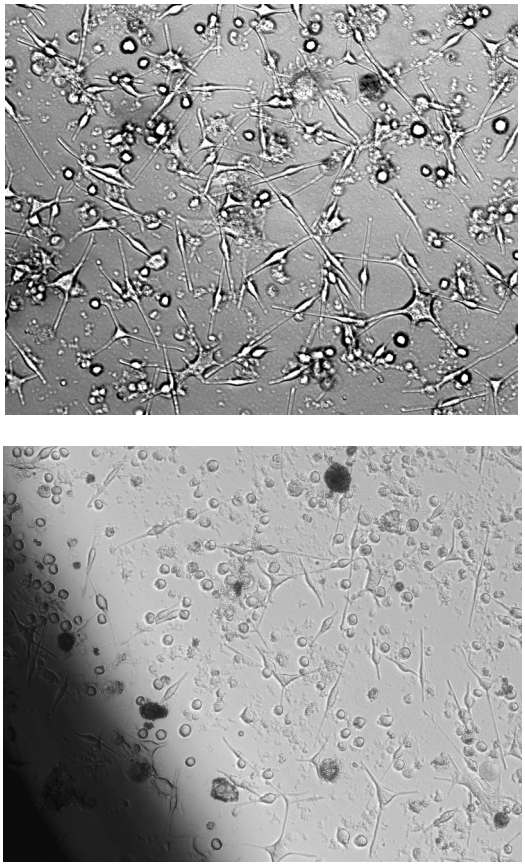

Fig. 8. Fibroblast cells partially proliferated and covered scaffold surface, 48h after seeding.

ACKNOWLEDGEMENTS

The authors would like to thank Materials and Energy Research Center (MERC, P.O. Box 31787-316, Karaj, Iran) for partial financial support and Dr. Shamshiri for his help in cell attachment evaluation.

REFERENCES

1. Langer, R.S. and Vacantri, J.P. (1999) Tissue engineering: The challenges ahead. *Sci. Am. 280: 86-89.*
2. Gineste, L., Gineste, M., Ranz, X., Ellefterion, A., Guilhem, A., Rouquet, N. and Frayssinet, P. (1999) Degradation of hydroxyapatite, fluoroapatite, and

[Downloaded from ibj1.pasteur.ac.ir on 2026-10-20]

[DOR: 20.1001.1.1028852.2006.10.4.8.3]

fluorohydroxyapatite coatings of dental implants in dogs. *J. Biomed. Mater. Res. 48: 224-234.*

3. Sonju Clasen, A.B. and Ruyter, I.E. (1997) Quantitative determination of type A and type B carbonate in human deciduous and permanent enamel by means of Fourier transformation infrared spectroscopy. *Adv. Dent. Res. 11: 523-527.*
4. Cerroni, L., Filocamo, R., Fabbri, M., Piconi, C., Caropresso, S. and Condo, S.G. (2002) Growth of osteoblast like cells on porous hydroxyapatite ceramics: an *in vitro* study. *Biomed. Eng. 19: 119-124.*
5. Wozney, J.M. and Rosen, V. (1998) Bone morphogenetic protein and bone morphogenetic protein gene family in bone formation and repair. *Clin. Orthop. Rel. Res. 346: 26-37.*
6. Suchanek, W. and Yoshimura, M. (1998) Processing and properties of hydroxyapatite-based biomaterials for use as hard tissue replacement implants. *J. Mater. Res. 13 (1): 94-117.*
7. Asashina, I., Watanabe, M., Sakurai, N., Mori, M. and Enomoto, S. (1997) Repair of bone defect in primate mandibule using a bone morphogenetic protein (BMP) hydroxyapatite collagen composite. *J. Med. Dent. Sci. 44: 63-70.*
8. Myung C.C., Ching-Chang, K., William H.D. (2003) Preparation of hydroxyapatite-gelatin nanocomposite. *J. Biomaterials. 24: 2853-2862.*
9. Rose, P.I. (1985) Gelatin. In: *Encyclopedia of Polymer Science and Technology*. (Kroschwitz, J.I., editor), Vol. 7, Wiley, New York, pp. 488-513.
10. Reddi, A.H. (1998) Role of morphogenetic proteins in skeletal tissue engineering and regeneration. *Natl. Biotechnol. 16: 247-252.*
11. Chevallay, B. and Herbage, D. (2000) Collagen-based biomaterials as 3D scaffold for cell cultures: applications for tissue engineering and gene therapy. *Med. Biol. Eng. Comput. 38: 211-218.*
12. Cooper, C.W. and Falb, R.D. (1971) Surgical adhesives. *Ann. NY. Acad. Sci. 146 (1): 218-224.*
13. Bigi, A., Panzavolta, S. and Roveri, N. (1988) hydroxyapatite gelatin films: a structural and mechanical characterization. *Biomaterials 19: 739-744.*
14. Anthony, A. and Robert, L. (2001) Methods of Tissue Engineering. ISBN: 0124366368, Academic Press, USA. pp. 505-511.
15. Whang, K., Thomas, C.K., Nuber, G. and Healy, K.E. (1995) A novel method to fabricate bioabsorbable scaffolds. *Polymer 36: 837-842.*
16. Healy, K.E., Whang, K. and Thomas, C.H. (1998) Method of fabricating emulsion freeze-dried scaffold bodies and resulting products. U.S. Patent 5,723,508.
17. Lin, F.H., Yao, C.H., Sun, J.S., Liu, H.C. and Huang, C.W. (1998) Biological effects and cytotoxicity of the composite composed of tricalcium phosphate and glutaraldehyde cross-linked gelatin. *Biomaterials 19: 905-917.*
18. Usta M., D.L. Piech, R.K. and MacCrone, Hillig W.B. (2003) Behavior and properties of neat and filled gelatins. *Biomaterials 24: 165-172.*
19. Paschalis, E.P., DiCarlo, E., Betts, E., Sherman, P., Mendelsohn, R. and Boskey, A.L. (1996) FTIR micro spectroscopy analysis of human osteonal bone. *Calcif. Tissue Int. 59: 480-487.*
20. Payne, K.J. and Veis, A. (1988) Fourier transform IR spectroscopy of collagen and gelatin solutions: deconvolution of the amide I band for conformational studies. *Biopolymers 27: 1749-1760.*
21. Curry, J.D. (1970) The mechanical properties of bone. *Clin. Orthop. Rel. Res. 73: 210-231.*
22. Hodgskinson, R. and Currey, J.D. (1986) Effect of variation in structure on Young's modulus of cancellous bone. A comparison of human and non human material. *Proc. Inst. Mech. Eng. [H] 204: 115-121.*
23. Hng, K.A., Best, S.M. and Bonfield, W. (1999) Characterization of porous hydroxyapatite. *J. Mater. Sci. 10: 135-145.*
24. Hodgkinson, R. and Curry, J.D. (2002) Effect of variation in structure on Young's modulus of cancellous bone. A comparison of human and non human material. *Proc. Inst. Mech. Eng. [H] 204: 115-121.*
25. Chang, M.C., Ikoma, T., Kikuchi, M. and Tanaka, J. (2002) Preparation of a porous hydroxyapatite-collagen nanocomposite using glutaraldehyde as a cross linking agent. *J. Mater. Sci. Lett. 20 (13): 1129-1201.*
26. Myung, C.C. and Junzo, T. (2002) FT-IR study for hydroxyapatite-collagen nanocomposite cross-linked by glutaraldehyde. *Biomaterials 23: 4811-4818.*
27. George, S. (2002) Infrared and Raman Characteristic Group Frequencies. 3th edition, ISBN: 0470093072, John Wiley & Sons, pp. 40-53.
28. Doyle, B.B. (1975) Infrared spectroscopy of collagen and collagen like polypeptides. *Biopolymers 14: 937-957.*
29. Epaschalis, E.P., Betts, E., DiCarlo, E., Mendelsohn, R. and Boskey, A.L. (1997) FTIR microspectroscopic analysis of normal human cortical and trabecular bone. *Calcif. Tissue Int. 61: 480-486.*
30. Michael A.K. (2004) Biomechanical considerations of animal models used in tissue engineering of bone. *Biomaterials 25: 1697-1714.*
31. Robert C.T., Michael J.Y., John M.P., Antonios G.M. (1998) Hydroxyapatite fiber reinforced poly (α-hydroxy ester) foams for bone regeneration. *Biomaterials 19: 1935-1943.*
32. Flatley, T.J., Lynch, K.L., Benson, M. (1983) Tissue response to implants of calcium phosphate ceramic in the rabbit spine. *Clin. Orthop. 179: 246-252.*
33. Hulbert, S.F., Morrison, J.S. and Klawitter, J.J. (1972) Tissue reaction to three ceramics of porous and non porous structures. *J. Biomed. Mater. Res. 6: 347-374.*

[Downloaded from ibj1.pasteur.ac.ir on 2026-10-20]

[DOR: 20.1001.1.1028852.2006.10.4.8.3]

34. Evans, L.A., Macey, D.J. and Webb, J. (1992) Calcium biomineralization in the regular teeth of the chiton, acanthopleura hirtosa. *Calcif Tissue Int. 51: 78-82*.
35. Hassna R.R., Miqin, Z. (2003) Preparation of porous hydroxyapatite scaffolds by combination of gel-casting and polymer sponge methods. *Biomaterials 24: 3293-3302*.
36. Spulveda, P., Ortega, F.S., Innocentini, M.D.M. and Pandolfelli, V.C. (2000) Properties of highly porous hydroxyapatite obtained by the gelcasting of foams. *J. Am. Ceram Soc. 83: 3021-3024*.
37. Kikuchi, M., Suestsugu, Y., Tanaka, J., Ito, S., Ichinose, S., Shiniyama, K., Hiraoka, Y., Mandai, Y. and Nakatani, S. (1999) The biomimetic synthesis and biocompatibility of self-organized hydroxyl-apatite/collagen composites. *Bioceramics 12: 393-396*.

[Downloaded from ibj1.pasteur.ac.ir on 2026-10-20]

[DOR: 20.1001.1.1028852.2006.10.4.8.3]